JOURNAL OF APPLIED PHYSICS VOLUME 96, NUMBER 1 1 JULY 2004

Elastic, piezoelectric, and dielectric properties of $0.58Pb(Mg_{1/3}Nb_{2/3})O_3$-$0.42PbTiO_3$ single crystal

Hu Cao[a] and V. Hugo Schmidt
Department of Physics, Montana State University, Bozeman, Montana 59717

Rui Zhang and Wenwu Cao
Material Research Institute, The Pennsylvania State University, University Park, Pennsylvania 16802

Haosu Luo
Shanghai Institute of Ceramics, Chinese Academy of Sciences 215 Chengbei Road, Jiading, Shanghai 201800, People's Republic of China

(Received 23 September 2003; accepted 29 February 2004)

The elastic, piezoelectric, and dielectric constants of $0.58Pb(Mg_{1/3}Nb_{2/3})O_3$-$0.42PbTiO_3$ (PMN-42%PT) were determined experimentally using combined resonance and ultrasonic methods. At room temperature the PMN-42%PT single crystal has tetragonal symmetry. The measured piezoelectric constant d_{33} is $\sim 260\times 10^{-12}$ C/N. The electromechanical coefficients k_{15}, k_{31}, k_{33}, and k_t are 0.80, 0.39, 0.78, and 0.62, respectively. From the measured material constants the orientational dependence of phase velocities and electromechanical coupling coefficients was calculated. The results showed the tetragonal crystal exhibits isotropy in the X-Y plane and k_{15}, k_{33}, and k_t reach their maxima in [001]. © *2004 American Institute of Physics.*
[DOI: 10.1063/1.1712020]

I. INTRODUCTION

Relaxor ferroelectrics, such as $Pb(Mg_{1/3}Nb_{2/3})O_3$ (PMN), $Pb(Sc_{1/3}Nb_{2/3})O_3$ (PSN), and $Pb(Zn_{1/3}Nb_{2/3})O_3$ (PZN) and their solid solutions with $PbTiO_3$ have come into prominence due to their ultra-high dielectric and piezoelectric properties[1–4] in contrast to the conventional piezoelectric ceramics. More recently, there is increased interest in the relaxor ferroelectric single crystals $x Pb(Mg_{1/3}Nb_{2/3})O_3$-$(1-x)PbTiO_3$ (PMN-PT), which have a broad composition range and possess very high electromechanical coupling coefficients, piezoelectric, and dielectric constants and field-induced strain response.[5] For instance, PMN-33%PT single crystals, which have a rhombohedral phase near the morphotropic phase boundary (MPB), possess large piezoelectric ($d_{33}\sim 2500$ pC/N), dielectric ($\epsilon_r\sim 5000-5500$), and electromechanical coupling coefficients ($k_{33}\sim 94\%$). This system shows a promising potential of producing higher sensitivity ultrasonic transducers with superior broadband characteristics,[6] large strain actuators, and other electromechanical devices.

At present, most people focus their interests on the domain engineered single crystals with different compositions near or away from MPB. These available complete physical property data of $0.67Pb(Mg_{1/3}Nb_{2/3})O_3$-$0.33PbTiO_3$,[7] $0.70Pb(Mg_{1/3}Nb_{2/3})O_3$-$0.30PbTiO_3$,[8] $0.955Pb(Zn_{1/3}Nb_{2/3})O_3$-$0.045PbTiO_3$,[9] and $0.92Pb(Zn_{1/3}Nb_{2/3})O_3$-$0.08PbTiO_3$ (Ref. 10) single crystals have been reported. However, more information is needed for us to understand and apply these materials. Therefore, the aim of this article is to provide a complete set of such data for the tetragonal $0.58Pb(Mg_{1/3}Nb_{2/3})O_3$-$0.42PbTiO_3$ single crystal. Practically, it is also very important to have a complete set of elastic, piezoelectric, and dielectric constants available. The data were obtained by using a combined method involving both pulse-echo and impedance resonance techniques.

A PMN-42%PT crystal, where the PT content is a little away from the MPB, has a tetragonal phase. For the tetragonal symmetry there are a total of 11 independent electroelastic constants: six elastic constants, three piezoelectric constants, and two dielectric constants to be determined.[11] The dielectric constants ϵ_{11}^T and ϵ_{33}^T were measured from the low frequency capacitance using the parallel capacitor approximation. The elastic compliance s_{11}^E and the electromechanical coefficient k_{31} can be calculated from the resonance and antiresonance frequencies of the length-extensional mode of vibration bars. Similarly, s_{33}^D and k_{33} can be calculated from the longitudinal extensional mode and c_{33}^D and k_t calculated from the thickness-extensional mode. Another five elastic constants c_{11}^E, c_{12}^E, c_{44}^E, c_{66}^E, and c_{44}^D were determined from the measured phase velocities of ultrasonic waves propagating along appropriate pure mode orientations. Using this measurement scheme, the only samples needed are those with the orientations of [001]/[010]/[001] and $[001/[110]/[1\bar{1}0]$. Thus, fewer samples are required when using this combined measurement technique.[12]

For each given wave propagation direction, the relationship between the phase velocity and associated material constants can be obtained by solving the Christoffel wave equations[13] and these velocities can be measured using the pulse-echo technique.[11] Other material constants can be derived from the piezoelectric constitutive equations and conversion formula.

[a]Electronic mail: caohu@hotmail.com

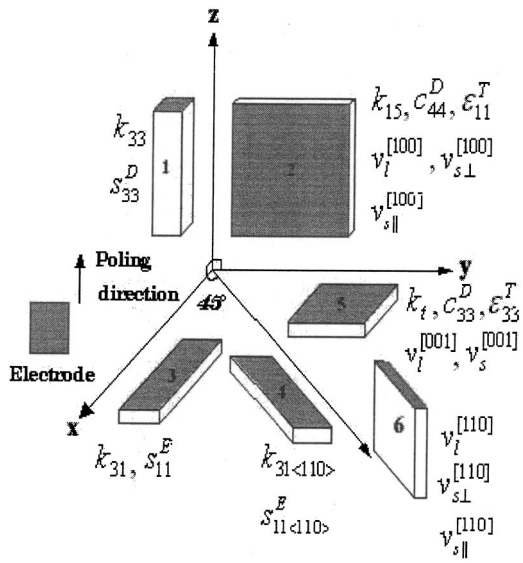

FIG. 1. The six types of test samples shown were cut from the PMN-0.42PT bulk single crystal and used to determine the whole set of material properties.

II. EXPERIMENTAL PROCEDURE

The $0.58Pb(Mg_{1/3}Nb_{2/3})O_3$-$0.42PbTiO_3$ single crystals were grown by the modified Bridgman method.[14] In the ferroelectric phase, the dipole in each cell of the PMN-42%PT crystals is along one of the six ⟨001⟩ directions. The as-grown crystals were cut along the pseudocubic crystallographic face [001] determined by a x-ray diffractometer. The impedance resonance and ultrasonic pulse-echo techniques, described in the IEEE standards on piezoelectricity,[11] are often used to characterize material properties for piezoelectric materials.[15,16] Because of segregation[17] during the process of crystal growth, the PT content in different parts in the crystal boule varies. Usually, 5%–10% PT composition variation is common in a large crystal. This will greatly affect the consistency of the measured data set. The Curie temperature approximately reflects the PT content in samples. Therefore, in order to guarantee consistency, samples were cut from the same part of a crystal boule and Curie temperature of samples was limited in the range of 190 °C±3 °C. Then, each sample, based on the requirement of different types of measurements, was cut and polished into a rectangular parallelepiped shape with three pairs of parallel surfaces, where dimensions and geometries were determined by IEEE standards. The final dimensions of the samples used for the ultrasonic measurements were $5\times5\times0.8$ mm^3. For the resonance vibration bars the aspect ratio of samples exceeded 5:1 in order to yield nearly pure resonance modes.[11] Two sets of samples were prepared for a consistency check. Gold electrodes were sputtered onto parallel surfaces of samples for poling. An external electric field of 5–8 kV/cm was applied at room temperature in silicone oil along the [001] direction of cubic axes to pole these samples.

A 15 MHz longitudinal wave transducer (Ultra Laboratories, Inc.) and a 20 kHz shear wave transducer (Panametrics) were used for the pulse-echo measurements. The electric pulses used to excite the transducer were generated by a Panametrics 200 MHz pulser/receiver, and the time of flight between echoes was measured by a Tektronix 460A digital oscilloscope. For the resonance measurements an HP 4194A impedance/gain-phase analyzer was employed to measure the resonance and anti-resonance frequencies of these resonators. Dielectric constants are determined by measuring capacitances of [100] and [001] oriented parallel plates. The capacitance was measured at 1 kHz using a Stanford Research System SR715 LCR meter. The density of the samples was determined by applying the Archimedes principle.

Dielectric properties as a function of temperature were determined using a multi-frequency *LCR* meter (HP 4284A). Polarization and strain hysteresis were plotted using a modified Sawyer-Tower circuit driven by a lock-in amplifier (Stanford Research System, Model SR830). (See Fig. 1.)

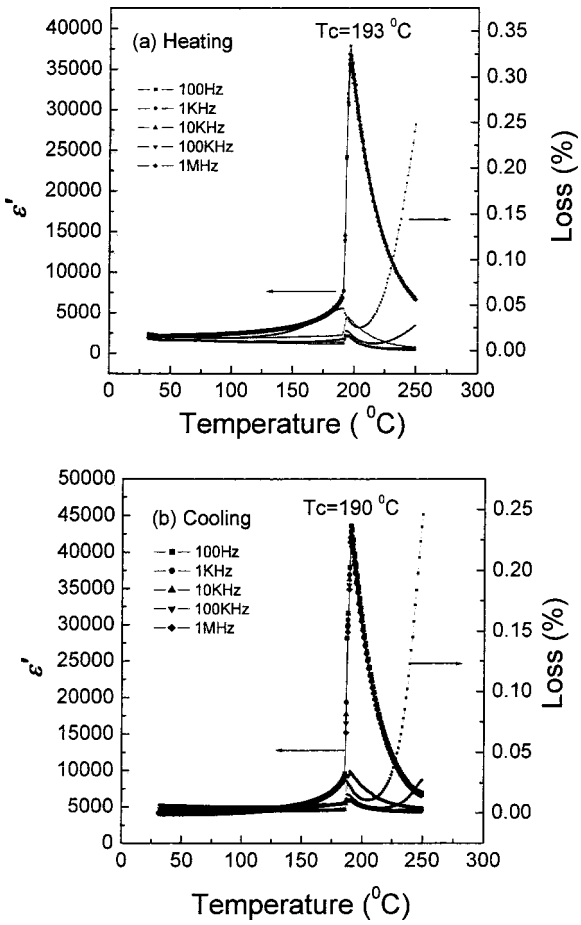

FIG. 2. Temperature and frequency dependence of dielectric constant ϵ_r and dielectric loss of [001]-oriented PMN-0.42PT on heating (a) and cooling (b).

III. RESULTS AND DISCUSSION

The dielectric constants ϵ_r and dielectric loss as a function of temperature and frequency for [001]-oriented PMN-42%PT on heating and cooling are presented in Fig. 2. The crystal exhibits very little frequency dispersion in the dielectric constants whether on heating or on cooling over the measured temperature range. The ϵ_r exhibits a sharp change near the transition temperature. Thus, PMN-42%PT is a normal

ferroelectric and possesses a first-order phase transition from the tetragonal ferroelectric phase to the cubic paraelectric phase.

There are marked rises in loss with increasing temperature above T_c at 1 kHz and especially at 100 Hz that can be attributed to thermally activated electrical conductivity. These rises are superimposed on the decreasing loss with increasing temperature just above T_c that are associated with the ferroelectric transition. To minimize effects of this transition-associated loss, an analysis based on Fig. 2(b) was made only in the 225 to 250 °C range in which the transition-associated loss is small. If one assumes that all dielectric loss in this range is due to conductivity, the appropriate formulas are

$$\sigma' = \epsilon_0 \epsilon'' \omega; \quad \epsilon'' = 0.01 \epsilon' (\text{loss}\%).$$

Here, σ' is the real part of the conductivity, ϵ'' is the lossy part of the permittivity, and ω is the angular frequency. Upon plotting the conductivity found from the 100 Hz data against inverse temperature over the above temperature range, a straight line is obtained that gives a conductivity of 1.55×10^{-8} S/m at 500 K (227 °C) with an activation energy of 0.79 eV and a preexponential coefficient $\sigma_0 = 1.44$ S/m. Such conductivity is a common feature of perovskite crystals and ceramics.[18] For instance, a $SrTiO_3$ (also perovskite) single crystal measured by Schmidt *et al.* showed conductivity at 500 K and 100 Hz of 4.15×10^{-7} S/m and comparable activation energy, with a weak frequency dependence.[18] The conductivity plot for PMN-42%PT at 1 kHz showed curvature because of the residual transition-associated loss, but at the highest temperature the curve approached the slope of the 100 Hz data, with conductivity 10% higher than at 100 Hz. From this result, it can be concluded that the frequency dependence of the conductivity is no stronger than $f^{0.05}$.

Polarization hysteresis loops as a function of electric field, and strain versus electric field (bipolar) behavior for the [001]-oriented PMN-42%PT crystal are plotted in Figs. 3(a) and 3(b), respectively. The value of remnant polarization P_r is ~42 μC/cm^2 and the coercive electric field E_c is 5.3 kV/cm when the maximum applied electric field is 13 kV/cm. Upon increasing the applied field the loop becomes "fatter" and E_c goes from 5.85 kV/cm for maximum field 16 kV/cm to 6.85 kV/cm for maximum field 20 kV/cm. However, the remnant polarization has almost no change in this range of applied fields. As [001] is the polar direction for PMN-42%PT, complete poling results in a single domain state, and piezoelectric strain behavior might be expected to be hysteresis free for [001] poled PMN-42%PT crystals. However, Fig. 3(a) shows that the crystal leaves the single-domain state even before the field falls to zero, so some piezoelectric hysteresis is expected even for small fields. For large fields, as shown in Fig. 3(b), the significant hysteresis together with high strain value (0.08% at 13 kV/cm) indicates considerable domain reorientation under bias. Similar to the polarization loops, the strain loops become "fatter" with increasing maximum field.

A complete set of elastic, piezoelectric, and dielectric constants of PMN-42%PT crystals is listed in Table I. Material constants marked with "*" were determined directly by measurement and the others are indirectly derived quantities. The relevant constants of PMN-30%PT and PMN-33%PT are also listed in Table I for comparison. It is seen that the difference in elastic stiffness constants is very small between PMN-30%PT and PMN-33%PT. The same behavior was observed in PZN-4.5%PT and PZN-8%PT crystals.[10] However, the difference is obvious compared to the PMN-42%PT crystals. The PMN-30%PT and PMN-33%PT crystals have rhombohedral phases at room temperature, while the PMN-42%PT has a tetragonal phase. Therefore, we can conclude that the structural difference has a significant influence on the elastic stiffness constants in the PMN-PT and PZN-PT systems. Similar phenomena were observed in the elastic compliance constants s_{ij}^D.

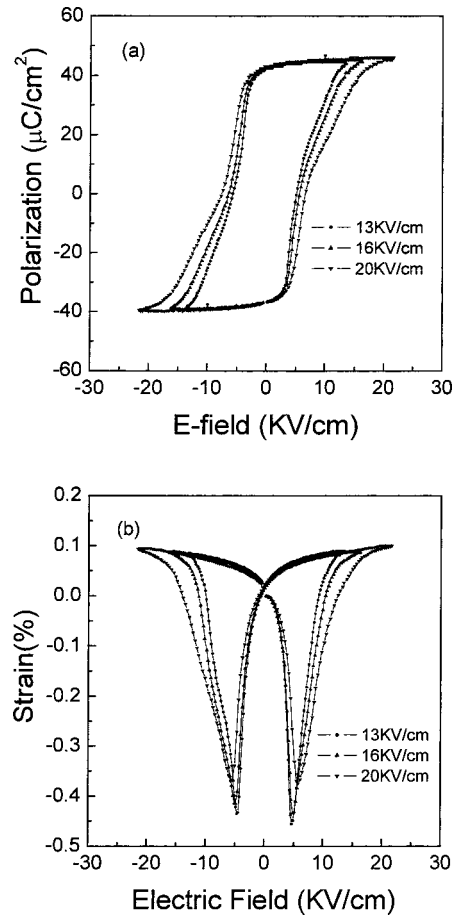

FIG. 3. Polarization (a) and strain (b) vs *E*-field (bipolar) curves for PMN-0.42PT crystals oriented along [001]. The maximum electric field is 13, 16, and 20 kV/cm, respectively.

The relationships between the measured phase velocities and related elastic constants were derived from the Christoffel wave equations, and these relationships and measured parameters are listed in Table II. For a crystal with 4 mm symmetry, sound velocities can be directly measured from eight independent pure modes. From each measurement, either one elastic constant or a linear combination of several elastic constants can be obtained as shown in Table II. It is seen that c_{44}^D and c_{12}^E can be determined by more than one measurement, which provides a control check. The difference between the measured phase velocity $v_{s\parallel}^{[100]}$ in the sec-

TABLE I. Measured and Derived Material Properties of PMN-42%PT Single Crystal Poled Along [001].

	Elastic stiffness constants: c_{ij} (10^{10} N/m^2)											
PT (%)	c_{11}^{E*}	c_{12}^{E}	c_{13}^{E}	c_{33}^{E}	c_{44}^{E*}	c_{66}^{E*}	c_{11}^{D}	c_{12}^{D}	c_{13}^{D}	c_{33}^{D*}	c_{44}^{D*}	c_{66}^{D}
42	17.51	8.51	8.3	10.5	2.85	8.0	17.7	8.7	7.18	16.99	8.05	8.0
33	11.5	10.3	10.2	10.3	6.9	6.6	11.7	10.5	9.0	17.4	7.7	6.6
30	11.7	10.3	10.1	10.8	7.1	6.6	11.8	10.4	9.5	17.4	7.8	6.6
	Elastic compliance constants: s_{ij} (10^{-12} m^2/N)											
PT (%)	s_{11}^{E*}	s_{12}^{E}	s_{13}^{E}	s_{33}^{E}	s_{44}^{E}	s_{66}^{E}	s_{11}^{D}	s_{12}^{D}	s_{13}^{D}	s_{33}^{D*}	s_{44}^{D}	s_{66}^{D}
42	9.43	−1.68	−6.13	19.21	35.09	12.5	8.02	−3.10	−2.08	7.64	12.42	12.5
33	69.0	−11.1	−55.7	119.6	14.5	15.2	44	−34	−4.1	11.1	13.0	15.2
30	52.0	−18.9	−31.1	67.7	14.0	15.2	39.7	−31.2	−4.7	10.8	12.9	15.2
	Piezoelectric constants: e_{ij} (C/m^2) d_{ij} (10^{-12} C/N) g_{ij} (10^{-3} Vm/N) h_{ij} (10^8 V/m)											
PT (%)	e_{15}	e_{31}	e_{33}	d_{15}	d_{31}	d_{33}^{*}	g_{15}	g_{31}	g_{33}	h_{15}	h_{31}	h_{33}
42	37.50	−2.1*	12.2	131	−91	260	17.23	−15.57	44.5	13.87	−9.16	53.22
33	10.1	−3.9	20.3	146	−1330	2820	10.3	−18.4	38.8	7.9	−5.9	33.7
30	13.6	−2.4	27.1	190	−921	1981	6.0	−13.3	28.7	4.6	−2.2	24.6
	Dielectric constants: $\epsilon(\epsilon_0)$, $\beta(10^{-4}/\epsilon_0)$ electromechanical coupling constants											
PT (%)	ϵ_{11}^{S}	ϵ_{33}^{S}	ϵ_{11}^{T*}	ϵ_{33}^{T*}	β_{11}^{S}	β_{33}^{S}	β_{11}^{p}	β_{33}^{T}	k_{15}^{*}	k_{31}^{*}	k_{33}^{*}	k_{t}^{*}
42	3054	259	8627	660	3.27	38.61	1.16	15.15	0.8	0.39	0.78	0.62
33	1434	680	1600	8200	7.0	14.7	6.3	1.2	0.32	0.59	0.94	0.64
30	3307	1242	3600	7800	3.0	8.0	2.8	1.3	0.29	0.49	0.92	0.62

[a]Measured properties.
[b]Density: $\rho=8.10\times10^3$ kg/m^3 (PMN-42%PT), $\rho=8.06\times10^3$ kg/m^3 (PMN-33%PT),[7] $\rho=8.04\times10^3$ kg/m^3 (PMN-30%PT).[8]

ond cut and $v_{s\parallel}^{[110]}$ in the sixth cut in Fig. 1 is very small and the corresponding elastic stiffness constants c_{44}^{D} are nearly equivalent, 7.93×10^{10} and 8.13×10^{10} N/m^2, respectively. According to the relationship in Table II, c_{12}^{E} can be separately determined by two equations and the corresponding calculated values of c_{12}^{E} are 8.4×10^{10} and 8.8×10^{10} N/m^2. The elastic stiffness constants c_{44}^{D} and c_{44}^{E} are calculated from the measured phase velocities. The shear coupling coefficient 0.80 of k_{15} can be calculated by $k_{15}^2=1-c_{44}^{E}/c_{44}^{D}$. In order to test the consistency, the frequency constants 1987 m/s of $2tf_r$ (t is the thickness of sample and f the resonance frequency of sample) and 3901 m/s of $2tf_a$ in the thickness shear mode were measured and 0.798 of k_{15} can be calculated by $k_{15}^2=\pi f_r/2f_a \tan\{\pi(f_a-f_r)/2f_a\}$. The elastic stiffness constants c_{44}^{D} calculated from the ultrasonic method ($c_{44}^{D}\sim8.13\times10^{10}$ N/m^2) and from the impedance ($c_{44}^{D}\sim7.78\times10^{10}$ N/m^2) method differ slightly. Similarly, $c_{33}^{D}=16.8\times10^{10}$ N/m^2 from the ultrasonic measurement and 17.1×10^{10} N/m^2 from the resonance measurement. Also, a resonance bar with its long dimension in [110] and thickness in [001] was made to verify the consistency. From the measured frequency constants 4182 m/s of $2lf_r$ (l is the length of sample) and 4428 m/s of $2lf_a$ in length-extension mode along [110] $k_{31\langle110\rangle}$ of 0.365 can be calculated by $(k_{31}^2-1)/k_{31}^2=\tan\{(\pi/2)(f_a/f_r)\}/(\pi/2)(f_a/f_r)$ and the corresponding elastic compliance constant $s_{11\langle110\rangle}^{E}$ is 7.06×10^{-12} m^2/N. We have easily gotten s_{11}^{E}, s_{66}^{E}, c_{11}^{E}, c_{12}^{E}, and c_{66}^{E}. There are two sets of data to calculate s_{12}^{E}. One is $s_{11\langle110\rangle}^{E}=(s_{11}^{E}+s_{12}^{E})/2+s_{66}^{E}/4$ and the other is $s_{12}^{E}=s_{11}^{E}-1/(c_{11}^{E}-c_{12}^{E})$. Here we test the consistency by the combination of ultrasonic and impedance techniques again. First, -1.56×10^{-12} m^2/N for s_{12}^{E} can be calculated from the elastic compliance constants in the resonance measurement. However, -1.67×10^{-12} m^2/N of s_{12}^{E} can be calculated from the stiffness constants in the ultrasonic method. The difference of s_{12}^{E} separately obtained by the two methods is small. Therefore, the combination of ultrasonic and impedance techniques provides an effective way to measure the material property constants.

For the PMN-PT and PZN-PT systems the piezoelectric properties of rhombohedral crystals are much higher than those of tetragonal crystals. It is known that the piezoelectric constant d_{33} of PZN-PT and PMN-PT systems increases nonlinearly and very drastically near the MPB. When the PT content in crystals is much higher than that near the MPB, the value of d_{33} is smaller. For example, the piezoelectric constants d_{33} (measured for small fields) of PMN-33%PT and PMN-30%PT are much higher than 260×10^{-12} C/N of PMN-42%PT. This significant difference can be attributed to the engineered-domain configuration. For rhombohedral crystals the spontaneous polarization is along $\langle111\rangle$. There are eight possible polarization orientations for $\langle111\rangle$ domains. When poling is done by applying an electric field along the [001] direction only four of the eight possible polarization orientations remain, i.e., [111], $[\bar{1}11]$, $[1\bar{1}1]$, and $[\bar{1}\bar{1}1]$. Therefore, the components of all four polarization vectors along [001] are equal, so that the domain walls have no incentive to move under an external electric field along

TABLE II. The relationships between measured phase velocities of ultrasonic waves and elastic constants in a PMN-42%PT crystal poled along [001].

v	$v_l^{[001]}$	$v_s^{[001]}$	$v_l^{[100]}$	$v_{s\perp}^{[100]}$	$v_{s\parallel}^{[100]}$	$v_l^{[110]}$	$v_{s\perp}^{[110]}$	$v_{s\parallel}^{[110]}$
Velocity (m/s)	4551	1830	4653	3138	3129	5110	2380	3168
$\rho v^2=$	c_{33}^{D}	c_{44}^{E}	c_{11}^{E}	c_{66}^{E}	c_{44}^{D}	$(c_{11}^{E}+c_{12}^{E}+2c_{66}^{E})/2$	$(c_{11}^{E}-c_{12}^{E})/2$	c_{44}^{D}

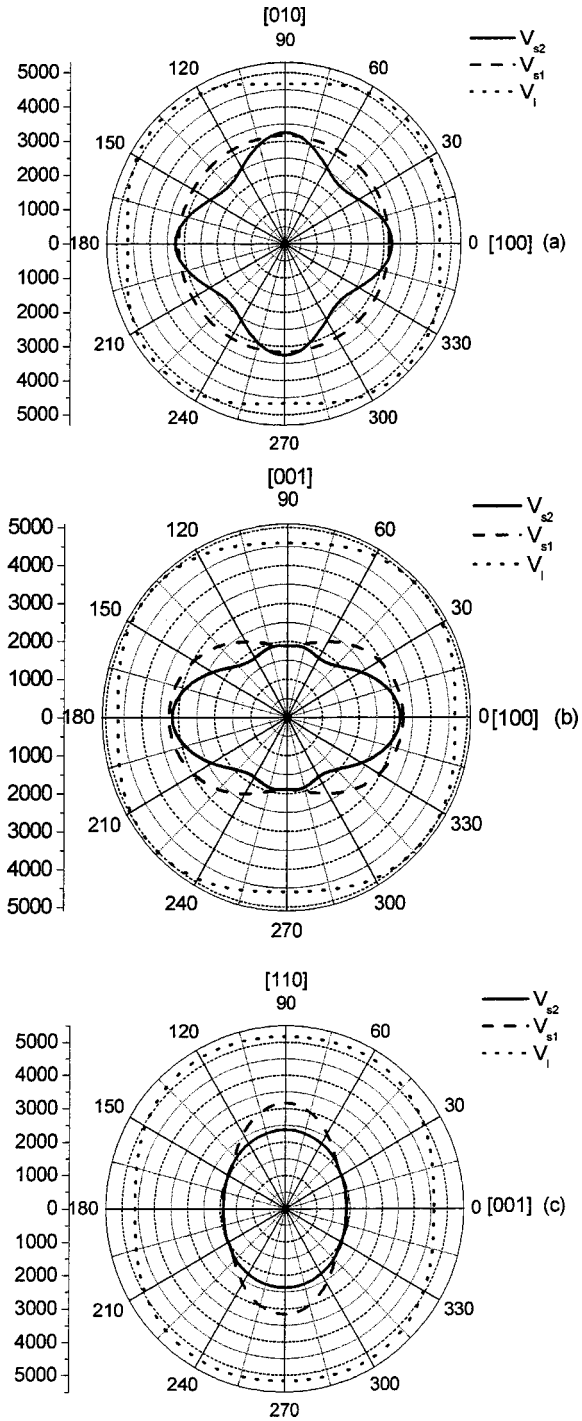

FIG. 4. Orientational dependence of the longitudinal velocity v_l and the two shear velocities v_{s1} and v_{s2} in (a) the [100]-[010] plane, (b) the [100]-[001] plane, and (c) the [110]-[001] plane.

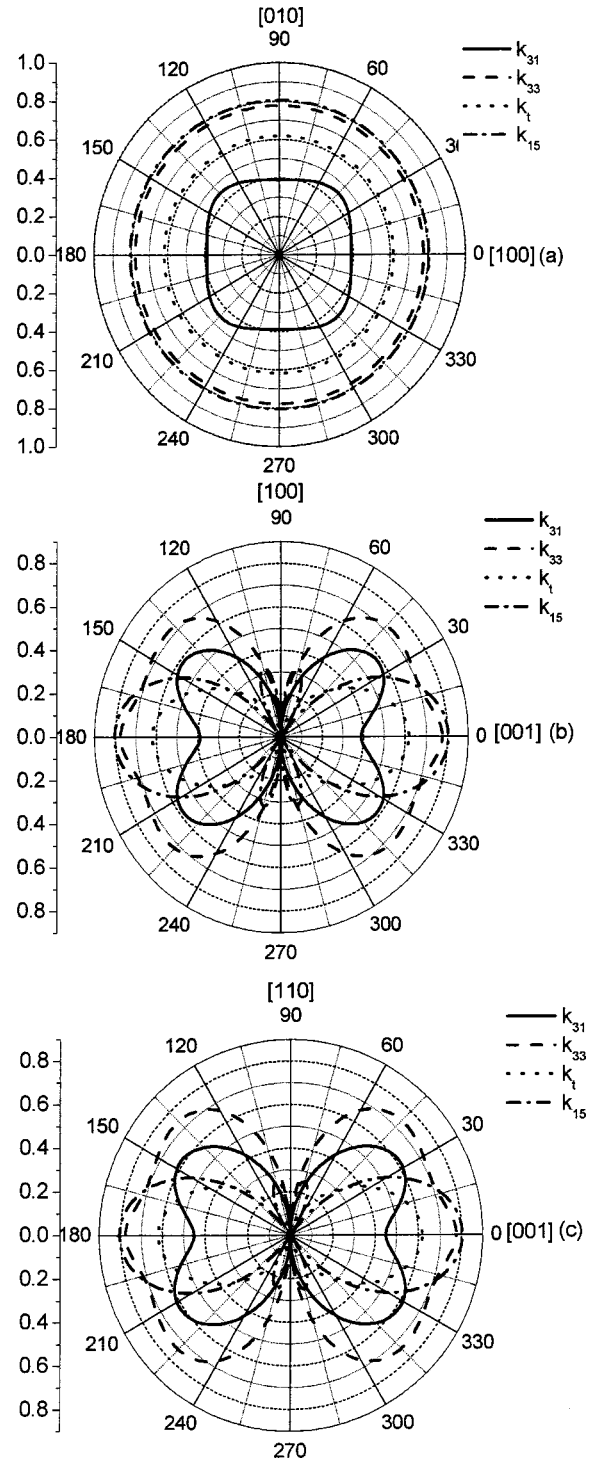

FIG. 5. Orientational dependence of the coupling coefficients k_{15}, k_{33}, k_t, and k_{31}, in (a) the [100]-[010] plane, (b) the [100]-[001] plane, and (c) the [110]-[001] plane.

[001]. However, the domains can change shape by both shearing and stretching, causing the piezoelectric constant to exhibit a high value. In contrast, the polarization is mostly along [001] in a [001] poled tetragonal crystal and the field can only cause stretching of the [001] domain, but not shearing, so the piezoelectric constant is lower.

According to the electromechanical coupling coefficients listed in Table II, k_{33} of rhombohedral crystals is much larger than that of tetragonal crystals. However, k_t is almost equal for rhombohedral and tetragonal crystals. The orientation dependence of the phase velocities and electromechanical coupling coefficients of PMN-42%PT single crystal based on the measured material constants in Table I is plotted in Figs. 4 and 5. Figure 4 provides the directional dependence of phase velocities for sound waves propagating in the (a) X-Y, (b) Y-Z, and (c) [110]-Z planes. The calculated results reveal that the velocities of the longitudinal waves do not change with orientation as much as those of the shear waves. As

shown in Fig. 4(a), the shear wave propagation in the X-Y plane and polarized in the same plane has the strong orientational dependence. It has a maximum in [100] and a minimum in [110], respectively. Figure 5 presents the orientational dependence of the electromechanical coupling coefficients k_{15}, k_{31}, k_{33}, and k_t. In the X-Y plane the coefficients k_{15}, k_{33}, and k_t are isotropic and in the X-Z plane k_{15}, k_{33}, and k_t reach maxima in [001]. When poling is done along [001] the switching of 90° domains causes the lattice elastic energy to increase, however, resulting in a slight depoling after removing the applied field. Statistically, the remaining domains along [100] or [010] have an equal probability, which means the tetragonal PMN-42% crystal is isotropic in the X-Y plane. Therefore, the electromechanical coefficients exhibit isotropy and the situation in the [110]-[001] plane is very similar to that in the [010]-[001] plane as shown in Figs. 5(b) and 5(c). However, k_{31} has a slight change with orientation, which is possibly caused by the incomplete single domain state.

IV. SUMMARY AND CONCLUSION

The material properties of a $0.58Pb(Mg_{1/3}Nb_{2/3})O_3$-$0.42PbTiO_3$ single crystal poled in the [100] direction of original cubic axes were measured using a combined method of ultrasonic and resonance techniques. A complete set of elastic, piezoelectric, and dielectric constants for tetragonal PMN-42%PT was obtained. It was confirmed that the tetragonal PMN-PT system has lower piezoelectric constants compared to the rhombohedral PMN-PT system. The piezoelectric constant d_{33} is 260×10^{-12} C/N and the electromechanical coefficient k_{33} is 0.78. Based on the measured material constants, orientational dependence of phase velocities of ultrasonic waves propagating in the X-Y, Y-Z, and [110]-Z planes and of the electromechanical coupling coefficients has been analyzed. It was observed that the anisotropy of phase velocities is strong for the shear wave, whereas it is relatively weak for the longitudinal wave. For the electromechanical coupling coefficients the crystal exhibits isotropy in the X-Y plane and k_{15}, k_{33}, and k_t reach their maxima at [001]. However, because of the incomplete single domain status k_{31} has a slight variation with orientation.

ACKNOWLEDGMENTS

This research was sponsored by the Department of Defense under Grant No. N00014-02-1-0657. Crystals used for this study were provided by Dr. Haosu Luo at Shanghai Institute of Ceramics, Chinese Academy of Sciences. The measurement was performed at the Ultrasonic Lab at Pennsylvania State University.

[1] J. Kuwara, K. Uchino, and S. Nomura, Ferroelectrics **37**, 579 (1981).
[2] S. E. Park and T. R. Shrout, Mater. Res. Innovations **1**, 20 (1997).
[3] T. R. Shrout, Z. P. Chang, N. Kim, and S. Markgraf, Ferroelectr., Lett. Sect. **12**, 63 (1990).
[4] Y. Yamashita, Jpn. J. Appl. Phys., Part 1 **33**, 5328 (1994).
[5] S. E. Park and T. R. Shrout, IEEE Trans. Ultrason. Ferroelectr. Freq. Control **44**, 1140 (1997).
[6] S. Saitoh, T. Takeuchi, T. Kobayashi, K. Harada, S. Shimanuki, and Y. Yamashita, IEEE Trans. Ultrason. Ferroelectr. Freq. Control **46**, 414 (1999).
[7] R. Zhang, B. Jiang, and W. Cao, J. Appl. Phys. **90**, 3471 (2001).
[8] R. Zhang, W. Jiang, B. Jiang, and W. Cao, *Fundamental Physics of Ferroelectrics* (American Institute of Physics, New York, 2002), p. 188.
[9] J. H. Yin, B. Jiang, and W. Cao, IEEE Trans. Ultrason. Ferroelectr. Freq. Control **47**, 285 (2000).
[10] R. Zhang, B. Jiang, W. Jiang, and W. Cao, IEEE Trans. Ultrason. Ferroelectr. Freq. Control **49**, 1622 (2002).
[11] ANSI/IEEE STD. 176-1987, *IEEE Standard on Piezoelectricity* (IEEE, New York, 1987).
[12] S. Zhu, B. Jiang, and W. Cao, Proc. SPIE **154**, 3341 (1998).
[13] B. A. Auld, *Acoustic Fields and Waves in Solids* (Wiley, New York, 1973).
[14] H. Luo, G. Xu, P. Wang, and Z. Yin, Ferroelectrics **231**, 97 (1999).
[15] A. W. Warner, M. Onoe, and G. A. Coquin, J. Acoust. Soc. Am. **42**, 1223 (1967).
[16] J. Kushibiki and I. Takanaga, J. Appl. Phys. **81**, 6906 (1997).
[17] H. Luo, G. Xu, and H. Xu, J. Appl. Phys. **39**, 5581 (2000).
[18] V. H. Schmidt, G. F. Tuthill, C.-S. Tu, T. V. Schogoleva, and S. C. Meschia, J. Phys. Chem. Solids **57**, 1493 (1996).